IEEE Access
Multidisciplinary | Rapid Review | Open Access Journal

Received 9 July 2023, accepted 27 July 2023, date of publication 1 August 2023, date of current version 9 August 2023.

Digital Object Identifier 10.1109/ACCESS.2023.3300377

RESEARCH ARTICLE

Real Time Screening and Trajectory Optimization of UAVs in Cluster Based on Improved Particle Swarm Optimization Algorithm

LEI SHENG, HAO LI, YINGCHUAN QI, AND MANHONG SHI
Air Force Early Warning Academy, Wuhan 430019, China

Corresponding author: Hao Li (afeu_li@163.com)

This work was supported in part by the National Natural Science Foundation of China (NSFC) under Grant 61502522.

ABSTRACT To solve the problem of selecting drones for passive positioning within unmanned aerial vehicle (UAV) swarm and optimizing corresponding trajectories. This article constructs a method for determining and optimizing the trajectory of UAVs based on an improved particle swarm optimization (PSO) algorithm. Firstly, the time difference of arrival (TDOA) positioning principle was introduced and corresponding algorithm models were organized. Afterwards, the objective function and constraint conditions for selecting drones and optimizing flight paths were designed. The correlation between the optimal solutions of the continuous time optimization problem is used to determine the UAV for positioning. This paper constructs the UAV determination process based on similarity screening. At the same time, combined with the characteristics of the problem to be optimized, the Particle Swarm Optimization (PSO) is improved from three aspects: updating the initial position of particles, improving the iteration formula and setting the adaptive termination condition. This paper further constructs the track optimization process based on improved particle swarm optimization. Through simulation experiments and algorithm comparison, it can be seen that the method constructed in this article can determine the drone used for positioning in real-time and optimize its spatial position. Compared to the selected drones and mainstream passive positioning methods, the method in this article reduces errors by more than 60% and 45%.

INDEX TERMS Particle swarm optimization, passive location, UAV swarm, trajectory optimization, time difference of arrival.

I. INTRODUCTION

As electromagnetic space has become the fifth-dimensional battlefield after ''land, sea, air, and sky'', the importance and research efforts of various countries in electromagnetic space have increased sharply. When using and radiating electromagnetic waves, equipment also exposes its own position, and passive location emerges as the times require [1], [2], [3], [4], [5]. The accuracy of passive positioning is highly correlated with the spatial position of the sensor. With the rapid development of drones, optimizing the spatial trajectory of drones for passive positioning has become a new way to improve positioning accuracy.

The current research on passive location can be divided into two main directions. The first is to study and improve the location accuracy algorithm. Such as improving time of arrival (TOA) [6], time difference of arrival (TDOA) [7], received signal strength (RSS) [8] and angle of arrival (AOA) [9], [10], etc. Since this article does not involve the improvement of the location algorithm, it will not be discussed too much here.

The second type of research mainly focuses on optimizing the layout of passive positioning stations. Mainly by designing various criteria to optimize the positions of localization points, thereby improving the accuracy of passive localization algorithms. Literature [11] deduced the optimal

The associate editor coordinating the review of this manuscript and approving it for publication was Cong Pu.

configuration of AOA positioning under different system errors based on the criterion of minimum Circular error probable (CEP). Geometric Dilution of Precision (GDOP) [12], [13] was the most widely used localization criterion. Literature [14] derived the optimal analytical solution of TOA based on the GDOP criterion and quantified the positioning accuracy of different configurations. This derivation process is of great significance for related research. Literature [15] utilized the GDOP criterion to determine and optimize the sensor to be activated at the next moment, thereby achieving optimal control decisions for the sensor and further improving positioning efficiency. Literature [16] taken GDOP as the objective function and optimizes the optimal configuration of the sensor under coherent or non-coherent signal conditions. This improves the positioning accuracy of the target. Literature [17] derived the optimal positioning configuration under the TDOA system using Cramer Rao Lower Bound (CRLB) as the criterion. Based on this, literature [18] further considered the impact of sensor measurement errors, and obtained the optimal positioning configuration under the TDOA system with correlated errors. Literatures [19] and [20] studied the joint CRLB for estimating target velocity and position, and thus obtained the optimal configuration for measuring target velocity and position. Literature [21] used particle swarm optimization (PSO) to optimize CRLB, and obtained the optimal angle direction under TDOA system. Literatures [22] and [23] both derived the optimal configurations under AOA and TOA positioning systems using Fisher Information Matrix (FIM) as the criterion.

One of the most obvious advantages of using drone clusters for passive positioning is that each drone can optimize and adjust its spatial position in real-time based on the target state, thereby improving positioning accuracy [24]. Literature [25] studied the feasibility of locating drone platforms loaded with TDOA sensors, which is of great significance for studying passive localization of drones. But only considering the drone cluster flying in a fixed configuration. The article did not study the impact of different configurations on positioning effectiveness. Literature [26] taken the determinant value of FIM as the optimization objective function, and optimizes the track of dual UAVs positioning static targets in RSS mode. Literature [27] was also based on the RSS, combining FIM with Kalman-filtering to optimize the positioning trajectory of unmanned aerial vehicles.

From the above literature, it can be seen that the current research on passive positioning mainly focuses on improving passive positioning methods and static station layout. By designing various criteria, the accuracy of passive localization algorithms can be improved. Or study the optimal station configuration under different positioning systems. A few literature references involve using drone clusters to locate targets. By utilizing drone clusters, the position of each drone can be adjusted in real-time, thereby improving positioning efficiency. Especially, the methods mentioned in the above literature will be adaptively improved to solve the passive localization problem of unmanned aerial vehicle clusters. However, how to screen UAVs for positioning in real time according to the target state has become an important problem restricting the positioning efficiency. Therefore, this article conducts research.

The main work and contributions of this paper can be summarized as follows:

(1) This paper constructs a method of UAV screening and route optimization in UAV cluster, so as to realize the real-time scheduling of UAVs in the cluster and the optimal positioning of the target.

(2) This paper analyzes the characteristics of the continuous time UAV parameter optimization problem, and proposes the strategy of inheriting the optimization results to improve the optimization accuracy and reduce the time-consuming of the algorithm.

(3) Aiming at the continuous time optimization problem, this paper improves the particle swarm optimization algorithm from three aspects. Through simulation and standard function test, it can be seen that the improved algorithm has good optimization efficiency and faster speed.

This article takes drone clusters as the research object, optimizes and determines the drones used for positioning in real-time, and optimizes their next spatial position to improve positioning efficiency. Introduced the passive positioning principle of TDOA and established the corresponding measurement model in Section II. Designed the objective function and constraint conditions for selecting drones and optimizing flight paths, and provided the optimization process in Section III. Sort out the two characteristics of the problem to be optimized, and then improve the particle swarm algorithm in Section IV. Conduct simulation verification and algorithm comparison to highlight the advantages of the method in Section V. The final conclusion is drawn in Section VI.

II. LOCATION MODEL AND AND ERROR ANALYSIS OF UAV SWARM BASED ON TDOA

A. PRINCIPLES OF TDOA

TDOA location, also known as hyperbola location, is an important part of passive location. The principle is that the time difference occurs because different sensors receive the target emitter signal at different times. According to the time difference, the distance difference between the target and different sensors can be obtained. Thus, the position of the target can be estimated. That is, the position of the target can be obtained by measuring the time difference of the target signal reaching different sensors, as shown in Figure 1.

As shown in Figure 1, any two receivers determine a group of hyperbolas, and the intersection of multiple hyperbolas is the position of the target. Assuming the position of the i-th drone used for passive positioning is (x_i, y_i, z_i), $i = 0,1,2,3$. The target location is (x_t, y_t, z_t). Set r_i as the distance from the i-th drone to the target. Using 0-th drone as the main station, the basic equation set for TDOA positioning can

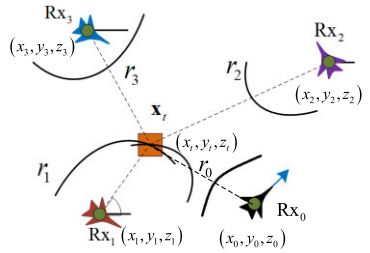

FIGURE 1. Schematic diagram of TDOA location.

be obtained as follows:

$$\begin{cases} r_0 = \sqrt{(x_t - x_0)^2 + (y_t - y_0)^2 + (z_t - z_0)^2} \\ r_i = \sqrt{(x_t - x_i)^2 + (y_t - y_i)^2 + (z_t - z_i)^2} \\ \Delta r_i = r_0 - r_i \end{cases} \tag{1}$$

Solve formula (1), and the result is the estimated value of the target.

B. MODEL SOLUTION BASED ON CHAN ALGORITHM

Use the Chan algorithm to solve formula (1). Firstly, organize formula (1) as follows:

$$(r_0 - \Delta r_i)^2 = r_i^2 \tag{2}$$

Expand and then simplify formula (2) to obtain:

$$(x_i - x_0)\, x_t + (y_i - y_0)\, y_t + (z_i - z_0)\, z_t = D_i + r_0 \Delta r_i \tag{3}$$

where,

$$D_i = \frac{1}{2}\left(x_i^2 + y_i^2 + z_i^2 - x_0^2 - y_0^2 - z_0^2 - \Delta r_i^2\right) \tag{4}$$

Then the formula (3) can be rewritten as:

$$\begin{bmatrix} x_1 - x_0 & y_1 - y_0 & z_1 - z_0 \\ x_2 - x_0 & y_2 - y_0 & z_2 - z_0 \\ x_3 - x_0 & y_3 - y_0 & z_3 - z_0 \end{bmatrix} \begin{bmatrix} x_t \\ y_t \\ z_t \end{bmatrix} = \begin{bmatrix} D_1 + r_0 \Delta r_1 \\ D_2 + r_0 \Delta r_2 \\ D_3 + r_0 \Delta r_3 \end{bmatrix} \tag{5}$$

Let,

$$A = \begin{bmatrix} x_1 - x_0 & y_1 - y_0 & z_1 - z_0 \\ x_2 - x_0 & y_2 - y_0 & z_2 - z_0 \\ x_3 - x_0 & y_3 - y_0 & z_3 - z_0 \end{bmatrix} \tag{6}$$

$$X = \begin{bmatrix} x_t \\ y_t \\ z_t \end{bmatrix} \tag{7}$$

$$F = \begin{bmatrix} D_1 + r_0 \Delta r_1 \\ D_2 + r_0 \Delta r_2 \\ D_3 + r_0 \Delta r_3 \end{bmatrix} \tag{8}$$

Then formula (5) can be rewritten as:

$$AX = F \tag{9}$$

Assume A is fully ranked, namely rank(A) =3. Using the pseudo inverse method to solve formula (9), it is obtained that:

$$X = \left(A^T A\right)^{-1} A^T F \tag{10}$$

Let,

$$B = \left(A^T A\right)^{-1} A^T = \begin{bmatrix} b_{11} & b_{12} & b_{13} \\ b_{21} & b_{22} & b_{23} \\ b_{31} & b_{32} & b_{33} \end{bmatrix} \tag{11}$$

The location of the target is:

$$\begin{cases} x_t = n_1 r_0 + m_1 \\ y_t = n_2 r_0 + m_2 \\ z_t = n_3 r_0 + m_3 \end{cases} \tag{12}$$

where,

$$n_j = \sum_{i=1}^{3} b_{ji} \Delta r_i \tag{13}$$

$$m_j = \sum_{i=1}^{3} b_{ji} D_i \tag{14}$$

Bring formula (12) into formula (1) and simplify it to obtain:

$$a_0 r_0^2 + a_1 r_0 + a_2 = 0 \tag{15}$$

where,

$$\begin{cases} a_0 = n_1^2 + n_2^2 + n_3^2 - 1 \\ a_1 = 2n_1 (m_1 - x_0) + 2n_2 (m_2 - y_0) + 2n_3 (m_3 - z_0) \\ a_2 = (m_1 - x_0)^2 + (m_2 - y_0)^2 + (m_3 - z_0)^2 \end{cases} \tag{16}$$

Then solve formula (15) to achieve the positioning of the target.

C. ERROR ANALYSIS

Differentiating the third equation in formula (1),

$$\begin{aligned} d(\Delta r_i) = {} & (c_{0x} + c_{ix})\, dx_t + \left(c_{0y} + c_{iy}\right) dy_t \\ & + (c_{0z} + c_{iz})\, dz_t + (k_i - k_0) \end{aligned} \tag{17}$$

where,

$$\begin{cases} c_{ix} = (x_t + x_i)/r_i \\ c_{iy} = (y_t + y_i)/r_i \\ c_{ix} = (x_t + x_i)/r_i \\ k_i = c_{ix} dx_i + c_{iy} dy_i + c_{iz} dz_i \end{cases} \tag{18}$$

Then the positioning error of the target can be expressed as:

$$dX_t = \begin{bmatrix} dx_t \\ dy_t \\ dz_t \end{bmatrix} \tag{19}$$

The error caused by UAV position can be expressed as:

$$dX_U = \begin{bmatrix} k_1 - k_0 \\ k_2 - k_0 \\ k_3 - k_0 \end{bmatrix} \tag{20}$$

The position relationship between the target and the drones is represented by C, which is:

$$C = \begin{bmatrix} c_{0x} - c_{1x} & c_{0y} - c_{1y} & c_{0z} - c_{1z} \\ c_{0x} - c_{2x} & c_{0y} - c_{2y} & c_{0z} - c_{2z} \\ c_{0x} - c_{3x} & c_{0y} - c_{3y} & c_{0z} - c_{3z} \end{bmatrix} \tag{21}$$

The error caused by the time difference is:

$$dY = \begin{bmatrix} d\Delta r_1 \\ d\Delta r_2 \\ d\Delta r_3 \end{bmatrix} = CdX_t + dX_U \tag{22}$$

By adjusting the spatial position of the drone, C can be fully ranked. The positioning error of the target obtained through pseudo inverse method is:

$$dX_t = \left(C^T C\right)^{-1} C^T \left(dY - dX_U\right) \tag{23}$$

Let,

$$B = \left(C^T C\right)^{-1} C^T = \left(b_{ij}\right)_{3\times 3} \tag{24}$$

Assuming the mean error Δr_i of measurement is 0, and the position error of each drone are independent of each other. The covariance of the positioning error is:

$$\begin{aligned} P &= E\left[dX_t dX_t^T\right] \\ &= B\left(E\left[dYdY^T\right] + E\left[dX_U dX_U^T\right]\right) B^T \end{aligned} \tag{25}$$

where,

$$E\left[dYdY^T\right] = \times \begin{bmatrix} \sigma^2_{\Delta r_1} & \eta_{12}\sigma_{\Delta r_1}\sigma_{\Delta r_2} & \eta_{13}\sigma_{\Delta r_1}\sigma_{\Delta r_3} \\ \eta_{21}\sigma_{\Delta r_2}\sigma_{\Delta r_1} & \sigma^2_{\Delta r_2} & \eta_{23}\sigma_{\Delta r_2}\sigma_{\Delta r_3} \\ \eta_{31}\sigma_{\Delta r_3}\sigma_{\Delta r_1} & \eta_{32}\sigma_{\Delta r_3}\sigma_{\Delta r_2} & \sigma^2_{\Delta r_3} \end{bmatrix} \tag{26}$$

$$\begin{aligned} E\left[dX_U dX_U^T\right] = & \\ & E\left[\begin{pmatrix} k_1 - k_0 \\ k_2 - k_0 \\ k_3 - k_0 \end{pmatrix} \begin{pmatrix} k_1 - k_0 & k_2 - k_0 & k_3 - k_0 \end{pmatrix}\right] \\ & = diag\left(\begin{bmatrix} c^2_{1x}\sigma^2_{x1} + c^2_{1y}\sigma^2_{y1} + c^2_{1z}\sigma^2_{z1} \\ c^2_{2x}\sigma^2_{x2} + c^2_{2y}\sigma^2_{y2} + c^2_{3z}\sigma^2_{z3} \\ c^2_{3x}\sigma^2_{x3} + c^2_{3y}\sigma^2_{y3} + c^2_{3z}\sigma^2_{z3} \end{bmatrix}^T\right) \\ & + \left(c^2_{0x}\sigma^2_{x0} + c^2_{0y}\sigma^2_{y0} + c^2_{0z}\sigma^2_{z0}\right) \times I_{3\times 3} \end{aligned} \tag{27}$$

where η_{ij} is the correlation coefficient between Δr_i and Δr_j. $\sigma_{\Delta r_i}$ represents the standard deviation of distance measurement error between 0-th drone and the i-th drone. σ^2_{xi} represents the variance of the error of the i-th drone in the X-axis direction, σ^2_{yi} and σ^2_{zi} are the same. Let:

$$P = [m_{lh}]_{3\times 3} \tag{28}$$

The positioning error of the target is:

$$\begin{cases} \sigma^2_{xt} = m_{11} \\ \sigma^2_{yt} = m_{22} \\ \sigma^2_{zt} = m_{33} \end{cases} \tag{29}$$

The positioning accuracy of the target can be expressed as:

$$\begin{aligned} GDOP &= \sqrt{trace\,(P)} \\ &= \sqrt{\sigma^2_{xt} + \sigma^2_{yt} + \sigma^2_{zt}} \end{aligned} \tag{30}$$

The trace(P) in formula (30) represents the sum of elements on the main diagonal of matrix P in formula (25).

According to formulas (25) - (27) and (30), it can be seen that the spatial position of the drone affects the positioning accuracy of the target. Therefore, the next section will analyze and study the impact of drone position.

D. THE INFLUENCE OF DRONE POSITION ON PASSIVE POSITIONING ACCURACY

It is assumed that the four UAVs adopt linear, Y-shaped, T-shaped and Cross-shaped spatial distribution respectively. In the four modes, the shortest distance between two UAVs is 40 kilometers, and the performance of passive positioning equipment is the same. The corresponding GDOP distribution is shown in Figure 2.

As can be seen from Figure 2, different configurations of UAV clusters have a great impact on positioning accuracy. When using drone clusters for passive localization of targets, the different configurations of the cluster have a significant impact on the accuracy of target localization.

At present, research mainly focuses on the static layout of passive positioning stations. How to select fixed positioning points to achieve optimal overall positioning efficiency. By using drone clusters to locate targets, the relative position between the drone and the target can be gradually adjusted based on the positioning results, thereby achieving gradual optimization. According to the status of each drone in the UAV cluster, the route of the corresponding UAV is selected and optimized.

Through the analysis in this section, in cases where the performance of positioning equipment is similar, the positioning accuracy is only related to the spatial configuration of the drone.

III. METHOD FOR SELECTING AND OPTIMIZING TRAJECTORY BASED ON OPTIMAL SOLUTION SIMILARITY SCREENING

A. OBJECTIVE FUNCTION

Assuming there are M drones, the position of the i-th drone at time t is $[x_i(t), y_i(t), z_i(t)]$. Meanwhile, due to the use of TDOA positioning, only four drones are required. Therefore,

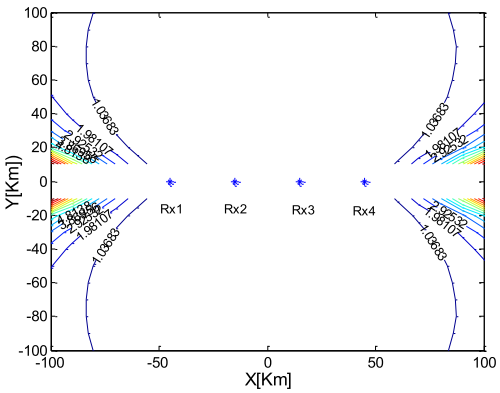

(a) linear

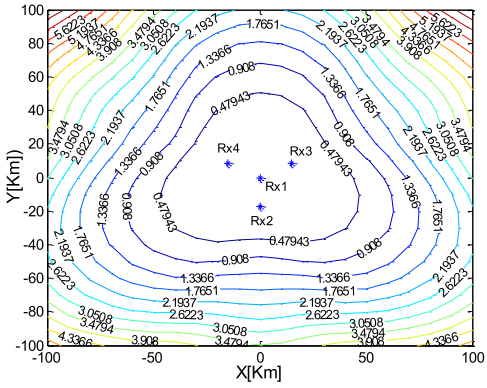

(b) Y-shaped

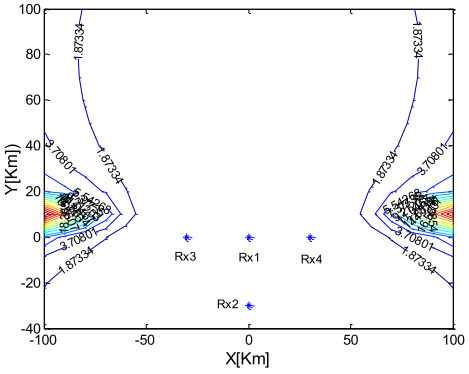

(c) T-shaped

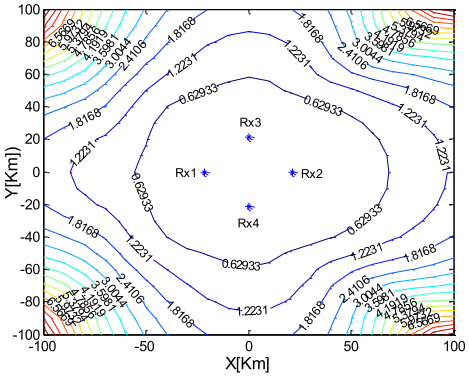

(d) Cross-shaped

FIGURE 2. Comparison diagram of GDOP under different distribution modes.

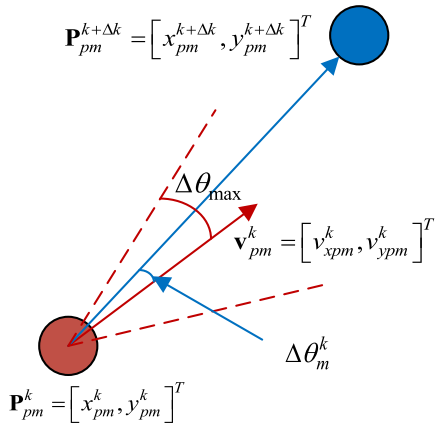

FIGURE 3. Schematic diagram of motion constraints.

it is necessary to select 4 drones from the M drones for passive positioning. According to the principle of arrangement and combination, it can be obtained that:

$$C_M^4=\frac{M\left(M-1\right)\left(M-2\right)\left(M-3\right)}{4\times3\times2}=CM \tag{31}$$

There are a total of CM selection methods. By optimizing these CM methods and ranking the results, the optimal scheme for positioning can be obtained.

Based on the idea of model predictive control (MPC). Set the objective function as:

$$F=\arg\min_{C_M^4}\left(\sum_{k=1}^{K}\gamma^k GDOP\left(t+k\right)\right) \tag{32}$$

where γ is the attenuation factor, k is the subsequent time, where $k=1,2,\ldots,K$.

The meaning of formula (32) is to select 4 drones from the M UAVs and optimize their spatial positions at the following K times, to minimize the sum of positioning errors.

Through the above process, the next moment of UAV motion parameters can be optimized. The following track can be obtained by continuously iterating the above process.

B. CONSTRAINT CONDITION

Constraints mainly include individual motion constraints and obstacle avoidance constraints, and cluster communication constraints and collision avoidance constraints.

It is assumed that the motion state of the UAV is at k and the next moment, that is, the motion state at the moment $k+\Delta k$is shown in Figure 3.

The position and speed of m-th UAV at time k are $\mathbf{P}_m^k=[x_m^k,y_m^k]$ and $\mathrm{v}_m^k=[v_{xm}^k,v_{ym}^k]$. Take it as the initial condition, optimize it to get the position and velocity at the next moment as $\mathbf{P}_m^{k+\Delta k}=[x_m^{k+\Delta k},y_m^{k+\Delta k}]$ and $\mathrm{v}_m^{k+\Delta k}=[v_m^{k+\Delta k},v_m^{k+\Delta k}]$. The corresponding relationship is shown in Figure 3. The

motion constraints should be satisfied, namely:

$$\begin{cases} \mathbf{P}_m^{k+\Delta k} = \mathbf{P}_m^k + \mathbf{v}_m^k \Delta k \\ \mathbf{v}_m^{k+\Delta k} = \mathbf{v}_m^k + \Delta \mathbf{v}_m^k \\ \left\| \mathbf{P}_m^{k+\Delta k} - \mathbf{P}_m^k \right\|_2 \le \left\| \mathbf{v}_m^k \right\|_2 \Delta k \end{cases} \tag{33}$$

$\|\|_2$means to take the 2-norm. Where $\Delta \mathbf{v}_m^k$ is the value of the velocity change, which should satisfy:

$$\begin{cases} \left\| \Delta \mathbf{v}_m^k \right\|_2 \le \Delta \mathrm{v}_{\max} \\ v_{\min} \le \left\| \mathbf{v}_m^{k+\Delta k} \right\|_2 \le v_{\max} \end{cases} \tag{34}$$

That is, the speed and the amount of speed change cannot exceed its allowable limit.

Similarly, the change amount $\Delta\theta_m^k$ of the UAV direction can be calculated according to the velocity vector at two moments, which should satisfy:

$$\left| \Delta \theta_m^k \right| \le \Delta \theta_{\max} \tag{35}$$

where || represents the absolute value.

The above are the motion constraints that the UAV should meet.

C. OPTIMIZATION PROCESS BASED ON SIMILARITY SCREENING

Due to the different positions of drones at each moment, the drones used to achieve optimal positioning may not necessarily be the same. At every moment, the drones used for positioning are selected based on the status information of the drones in the cluster, and their positioning efficiency is inevitably not inferior to the designated drones.

From formula (33), it can be seen that the parameters that need to be optimized are extremely complex and require a huge amount of computation. If C_M^4 optimization calculation is performed at every moment, the computational complexity is extremely high. But it is obvious that there must be some less effective or normal combination methods in the C_M^4 arrangement and combination. There is no need to further optimize and solve the formation.

Which combinations are worth further optimization and which do not require further calculation are the issues to be addressed in this section. Therefore, this section constructs an optimization process based on similarity filtering. As shown in Figure 4.

The optimization process in Figure 4 is divided into the 8 steps:

Step 1: Initialization time variable $t = 1$.

Step 2: Optimize the positioning results of a combination using an improved particle swarm optimization algorithm. Sort all combinations based on their positioning performance and execute the best results.

Step 3: Select the drone combination coordinates with positioning efficiency in the first K groups as an alternative solution set S. And then update the spatial locations of all drones. The four selected drones in the cluster perform corresponding optimization results, while the remaining drones remain in their original motion state.

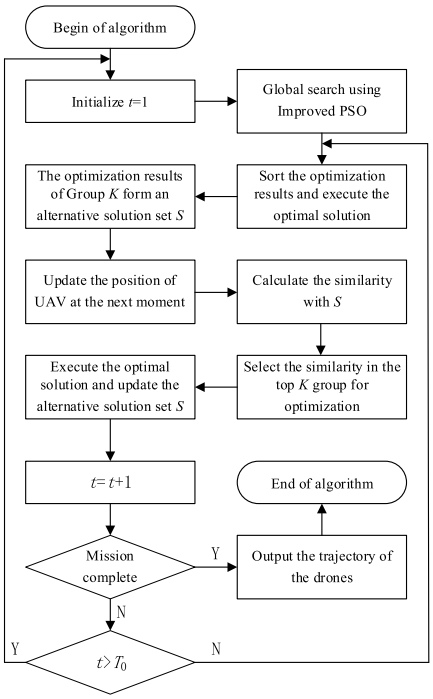

FIGURE 4. Algorithm flow.

Step 4: Using formula (36), calculate the similarity between the spatial position of the drone at the next moment and each set of solutions in the alternative solution set S.

$$R_{ij} = \sum_{i=1}^{4} \sqrt{\left(x_i - x_j\right)^2 + \left(y_i - y_j\right)^2 + \left(z_i - z_j\right)^2}, i \in C_M^4, \times j \in S \tag{36}$$

Step 5: Sort the similarity and select the top K groups for further search and optimization. Execute the optimal solution and update the alternative solution set S.

Step 6: Time variable t plus 1. Determine whether the task has ended. If it ends, execute Step 7; otherwise, execute Step 8.

Step 7: Output all optimization results. That is, the selected drone at each moment and its corresponding optimized position.

Step 8: Determine if t is approximately the set global update cycle T_0. If greater than, return to Step 1, otherwise, return Step 2.

At this point, the UAV number used for positioning at each time and the corresponding spatial position can be determined.

The improved particle swarm optimization algorithm in Step 2 will be introduced in the next section.

Calculating similarity in step 4 is inspired by static positioning. For static positioning, there is an optimal configuration, and the more similar it is to the optimal configuration,

the better its positioning effect. Therefore, the higher the similarity with the previous optimal positioning configuration, the more likely it is to achieve better positioning results. This is also the core of this optimization process.

Setting the global update cycle T_0 in Step 8 is to prevent the poor positioning effect of Type C_M^4 from causing large positioning errors. Because the subsequent optimization is based on the results of the pre-results. If the previous results are poor, the subsequent results will not be good. Therefore, after T_0 optimizations, it is necessary to conduct a global search again. If T_0 is set too large, if the first search result is not ideal, the subsequent T_0 will inherit the result, resulting in poor optimization effect. If T_0 is set too small, although it will reduce the possibility of the above problems, it will increase the calculation amount of the algorithm due to frequent global search. Therefore, t0 should be taken as appropriate. Let T_0 =10 later.

IV. IMPROVED PARTICLE SWARM ALGORITHM

A. PARTICLE SWARM ALGORITHM

Particle Swarm Optimization (PSO) is established by observing the predation characteristics of birds [28]. The algorithm is simple to operate and efficient to search, which has been widely used in many fields.

Assume that the dimension of the search space to be optimized is D, the total number of particles is N, and the total number of search iterations is T. Then the update iterative formula for optimization is:

$$v_{id}^{p+1} = \omega v_{id}^{p} + c_1 r_1 \left(p_{ibest}^{p} - x_{id}^{p}\right) + c_2 r_2 \left(p_{gbest}^{p} - x_{id}^{p}\right) \quad (37)$$

$$x_{id}^{p+1} = x_{id}^{p} + v_{id}^{p+1} \quad (38)$$

where $v_i^p = \left(v_{i1}^p, v_{i2}^p, \cdots, v_{iD}^p\right)$ represents the set of velocities of the i-th particle in each dimension during the t-th iteration, x_i^t represents the set of particle position, i = 1,2,…,N, d = 1,2,…,D, p = 1,2,…,P, ω is the inertia coefficient, c_1 and $c_2$are learning factors, r_1 and r_2 are random numbers uniformly distributed between [0, 1]. p_{ibest}^p and p_{gbest}^p are the best position in individual history and the best position in population history.

Then calculate the fitness function corresponding to the particle position. The better the fitness, the better the position of the particle. All particles adjust their speed direction and move towards a better position by comparing their fitness functions with other particles.

The above is the core formula and basic principle of the PSO algorithm.

Although PSO is fast, the problem to be optimized in this article is extremely complex. If we re optimize and calculate every time, it will waste computing resources and time.

Therefore, this article makes targeted improvements to the PSO based on the problems to be optimized.

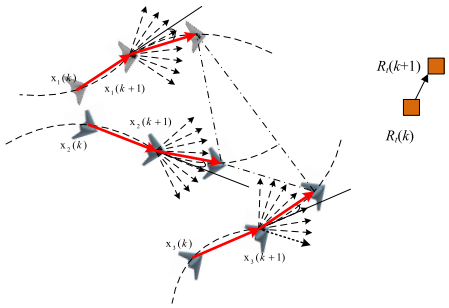

FIGURE 5. Changes in the positions of both parties at consecutive times.

B. CHARACTERISTICS OF THE PROBLEM TO BE OPTIMIZED

Assuming time k, the optimization result of UAV cluster and the subsequent motion state of the target are shown in Figure 5.

Combining Figure 5 and the motion constraints of the drone, it can be seen that the problem to be optimized has two characteristics. The first characteristic is that the position of each drone will not change significantly at two adjacent moments. When there is no significant change in the initial condition and objective function, the optimization results will not change significantly. Especially for the continuous time optimization problem to be optimized in this article. Inheriting the optimization results from the previous moment as the initial state of the next moment can significantly improve search efficiency.

The second characteristic is that in the process shown in Figure 4, K sets of optimization results are obtained for each optimization. All K optimization results may become the optimal solution. Therefore, in the optimization process of particle swarm optimization, if these optimization results can be utilized, it is of great significance to improve the optimization speed.

C. IMPROVED PARTICLE SWARM OPTIMIZATION ALGORITHM

In response to the above two characteristics, this article improves the PSO from three aspects.

1. Adjusting the initial position of particles for optimization at the next moment

According to the first characteristic of the problem to be optimized, which is that the initial conditions and optimization functions at adjacent times are relatively similar. The new optimal solution has a high probability of appearing near the optimal solution or suboptimal solution at the previous time. The combination of the optimal solution and the suboptimal solution is the alternative solution set S in the above.

Suppose the position of the m-th UAV at time t is $P_m(t)$ =$[x_m(t), y_m(t), z_m(t)]$. In order to ensure that the optimal solution can be found, CM-time optimization is required. Let S_{opt} be the optimal solution, $S_{\text{opt}} = S_{i,j,k,l}(t+1)$=$[P_i(t+1), P_j(t+1), P_l(t+1), P_{ik}(t+1)]$.

At this time, as long as the i-th, j-th, k-th, l-th UAV move to the optimized position, the optimal positioning of the target can be achieved.

At the same time, the optimization results of group CM are sorted. According to the optimization result, from the best to the worst, the sorting result is $S_{\text{all}} = [S_{\text{opt}}, S_2, S_3, \ldots, S_{CM}]$. Taking the first K solutions sorted in S_{all}, the alternative solution set $S = [S_{\text{opt}}, S_2, S_3, \ldots, S_K]$ can be obtained.

Therefore, in each optimization process, there is no need to randomly distribute the spatial positions of the initialized particle swarm within the feasible space. Just randomly distribute around the candidate solution set S, centered around the previous feasible solution. This will enable faster search for the target function.

As mentioned earlier, the number of solutions in the alternative solution set S is K, and the number of particles optimized is N. Since K is preset, N can be adjusted. Therefore, Z points are set at each solution for optimization, i.e. N=ZK.

Set the upper and lower limits of the d-th optimization dimension as $D_{d,max}$ and $D_{d,min}$. Divide this length into K segments, and generate initial particles near the k-th solution $x^d_{k,opt}$ of this dimension that meet:

$$x^d_m \in \left[x^d_{k,opt} - \frac{D_{d,\max} - D_{d,\min}}{2K}, x^d_{k,opt} + \frac{D_{d,\max} - D_{d,\min}}{2K} \right] \tag{39}$$

This ensures that the newly generated particles appear near the previous optimal solution.

2. Improving iterative formulas

The speed update in formula (37) of the PSO only considers the historical optimal and global optimal of this search. In the early stages of the search, both the historical optimal and the global optimal are relatively poor. At this point, the two optima have almost no guiding effect on the search, and even have a misleading effect. As the number of iterations increases, the role of these two optima becomes increasingly apparent until the algorithm converges.

The optimization results of the drone at the previous moment were obtained through numerous iterations. Although it was the solution from the previous moment. However, there was no significant change in the initial conditions and optimization objective function at this moment. The optimal solution from the previous moment has a significant impact on this optimization, especially in the initial stage, which is much greater than the global and historical optima of the particles in this optimization process. To achieve this, the optimal solution from the previous moment can be used to guide the initial stage of optimization.

The optimization results from the previous moment have a significant impact in the early stages of this search, but as the iteration progresses, the effectiveness should become increasingly weak. This avoids the optimization result from falling into the previous moment's optimal state. As the iteration progresses, the role of global and historical optima in this iteration should become increasingly apparent.

Let the total number of particle iterations be P, and according to the above discussion, adjust formula (37) to:

$$\begin{aligned} v^{p+1}_{id} = {} & \omega v^p_{id} + \frac{p}{P} c_l r_l \left(p^p_{ibest} - x^p_{id} \right) \\ & + c_g r_g \left(p^p_{gbest} - x^p_{id} \right) \\ & + \frac{P-p}{P} \sum_{k=1}^{K} c_k r_k \left(x^S_{k,opt} - x^p_{id} \right) \end{aligned} \tag{40}$$

Compared to formula (37), formula (40) incorporates the influence of the previous optimal solution. At the same time, a time adjustment factor was added before each item. Thus adjusting the degree of influence of different factors in different iterations. And then improve the speed of the algorithm.

3. Set adaptive termination conditions

The above two improvement points both improve the efficiency of the algorithm. And if the algorithm still undergoes P iterations, the total computational complexity of this algorithm increases instead of decreasing, and the efficiency of the algorithm will not be improved. To reduce the total time of algorithm operation, try to minimize the total number of iterations of the algorithm as much as possible. Therefore, it is necessary to set a new algorithm termination condition to stop searching when the particles converge, avoiding subsequent meaningless operations.

When the algorithm converges, the fitness function will not change. Let the change value of fitness function be ΔF,

$$\Delta F = \left| F_{fit}(p) - F_{fit}(p-q) \right| \tag{41}$$

where $F_{fit}(p)$ represents the corresponding fitness function value at iteration p. Due to the possibility of particles falling into local optima. When performing a few more iterations at this point, ΔF will not change. But at this point, the particles did not converge to the optimal solution. Therefore, when considering the change of fitness, it is necessary to increase the iteration gap when calculating the fitness function twice. Therefore, formula (41) introduces the constant q.

When the value of formula (41) is 0, the optimization can be terminated and the corresponding solution can be output.

By improving the above three aspects, the efficiency of the algorithm can be improved. At this point, the optimization process in Figure 4 can be used to determine the drone used for positioning and the corresponding spatial location for optimization in real-time.

V. SIMULATION AND VERIFICATION

A. PASSIVE LOCATION PERFORMANCE VERIFICATION AND ALGORITHM COMPARISON

To verify the performance of the localization algorithm proposed in this paper, the algorithm is compared with the localization method of the selected unmanned aerial vehicle, the method proposed in literature [2], literature [29] and literature [30].

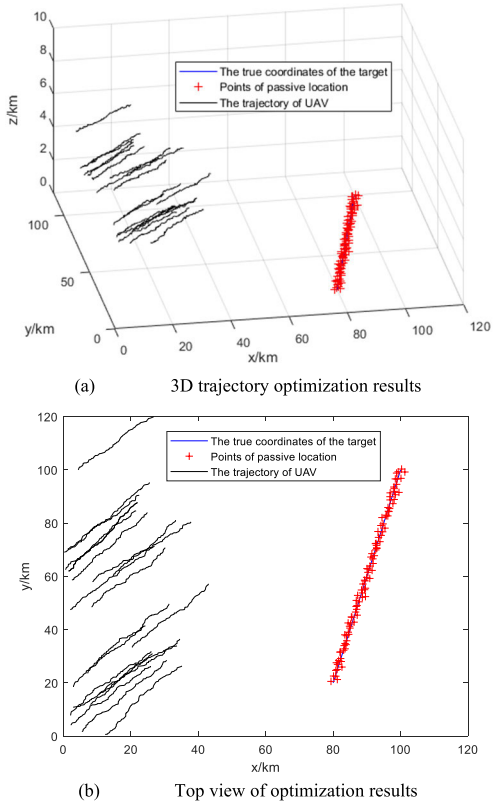

FIGURE 6. Optimization results of the algorithm in this paper.

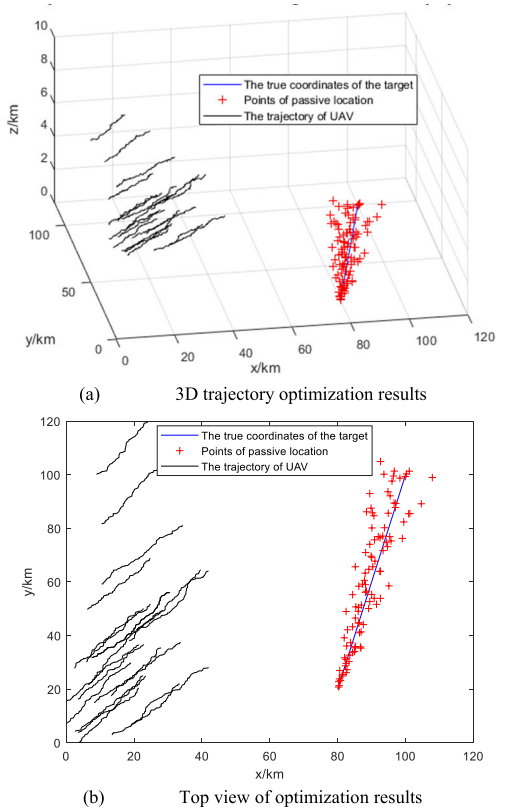

FIGURE 7. Optimization results of selected UAVs.

Our 20 drones were initially randomly distributed in an area with a horizontal axis of [0, 20] km and a vertical axis of [0,100] km, and the initial flight altitude is 5km. The speed limit is 30km/h. The initial position of the target is at (80, 20, 0) km, moving in a uniform straight line towards (100,100, 0) km. The target speed limit is 50km/h.

The particle swarm population is set to 6000, $c_1 = c_2 = 0.3$, the number of alternative solution sets S is set to 6, the upper limit of algorithm iteration times P is 10000, and the algorithm termination discrimination parameter $q = 200$.

Use the above five methods to locate the target. The other four methods, that is, the selected drone in the method of selecting drones, are the combination of drones with the best positioning effect after the first global search. Set a target movement for 100 minutes, positioning once every minute. The results obtained are shown in Figures 6- Figures 10.

By comparing the five sets of results in Figure 6- Figure 10, it is evident that the positioning effect of our method is superior to the other methods. The reason is that the method in this article selects the optimal drones for positioning, and tracking in real-time based on the target position. At the same time, according to the set objective function, the three-dimensional track of each UAV used for passive location is optimized to achieve the optimal location.

From Figure 7, it can be seen that as the target moves further away from the initial four drones used for positioning, the positioning effect deteriorates. This is because TDOA uses time difference for positioning. As the distance increases, there is no significant change in the distance difference. But the measurement error is positively correlated with the distance difference. As the target continues to move away, the measurement error will continue to increase. Ultimately, when there is no significant change in distance difference, the measurement error continues to increase, thereby affecting the measurement results. This is another reason why the performance of the method in Figure 7 is weaker than that in Figure 6.

It can be seen from Figure 8 that the results of the method in literature [29] are better than those in Figure 7. This is because literature [29] uses Doppler rate to improve the accuracy of moving target positioning. At the same time, CRLB is used as the objective function to optimize the configuration of UAV cluster. Therefore, compared with the classic TDOA method in Figure 7, the performance is improved. While, the performance of the method in literature [29] is still weaker than that in this paper. Firstly, literature [29] also adopts TDOA positioning mode, which has the shortcomings of TDOA discussed in the previous paragraph. Secondly, literature [29] only gives the final optimal configuration of UAV positioning. Without a detailed description of the positioning process, it is difficult to ensure the gradual optimization of the positioning process. Finally, the method in literature [29] does not consider the correlation of the target motion position, and only takes it as a single point positioning each time, which

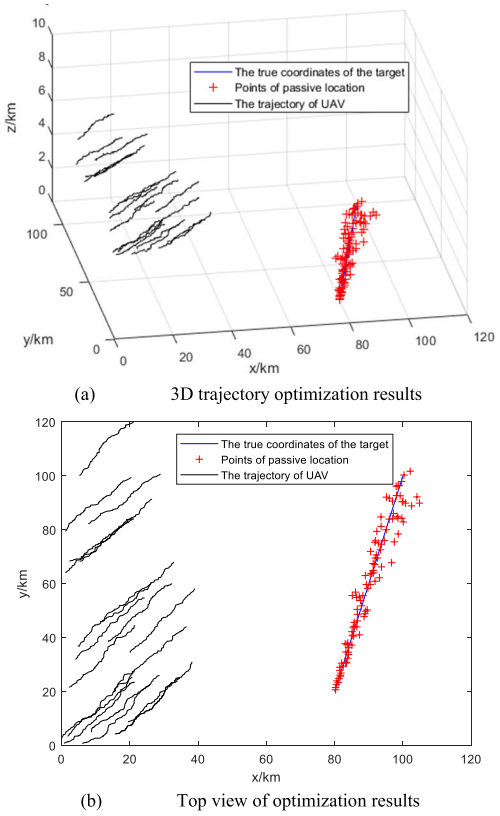

FIGURE 8. Optimization results of the algorithm in literature [29].

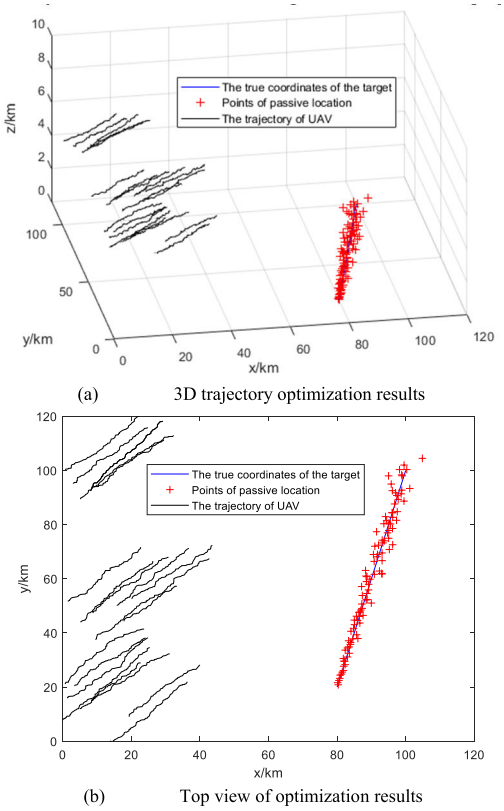

FIGURE 9. Optimization results of the algorithm in literature [2].

will also lead to an increase in error. However, due to the inheritance of the optimization results, this paper makes use of the correlation between the target positions to a certain extent. At the same time, the real-time location optimization method is given. Therefore, the performance of the method in this paper is better than that of the literature [29].

From Figure 9, it can also be seen that as the target moves, the positioning effect of the drone deteriorates. This is because [2] uses the received signal strength localization method (RSS). This method locates based on the difference in signal strength. Similarly, as the distance increases, the signal transmission distance increases. The receiving end receives a decrease in the strength of the signal itself, while the noise intensity remains almost unchanged. This leads to a decrease in the strength and signal-to-noise ratio of the receiving signal. This affects the positioning accuracy. Similarly, this is one reason why the method in Figure 9 is weaker than the method in this paper.

The method in Figure 10 is also based on RSS positioning mode, it also has the shortcomings discussed in the previous paragraph. Meanwhile, the research in literature [30] is similar to that in literature [29], and only the final positioning results are given. At the same time, the method in literature [30] does not consider the relevance of target motion. As a result, the performance of the method in literature [30] is weaker than that in this paper, and also weaker than that in literature [2].

In order to further quantify and compare the location performance. Under the condition that the simulation conditions remain unchanged, 50 Monte Carlo experimental simulations are carried out for each algorithm. Take the average value of the errors at each moment to obtain a comparison chart, as shown in Figure 11.

From Figure 11, it can be intuitively seen that over time. The positioning error of this algorithm is relatively stable and superior to the other four methods. This is because the method proposed in this paper can select the optimal combination of drones for positioning based on their spatial positions at different times. This ensures positioning accuracy. The other methods are increasingly affected by measurement errors due to the increasing distance difference between the drone and the target, resulting in a significant decrease in performance.

The reason why the method of literature [2] is superior to the other three methods is that literature [2] uses deep learning to predict the motion state of the target, so as to improve the positioning accuracy. However, due to the influence of increasing distance, the performance of the method is significantly reduced. The main reason why the method in literature [29] is better than that in literature [30] is that RSS is more sensitive to distance than TDOA. That is, the error of RSS increases with the distance, which is higher than that of TDOA. Therefore, the results in literature [29] are slightly better than those in literature [30]. At the same time, it can be seen that the positioning result of the selected UAV is not

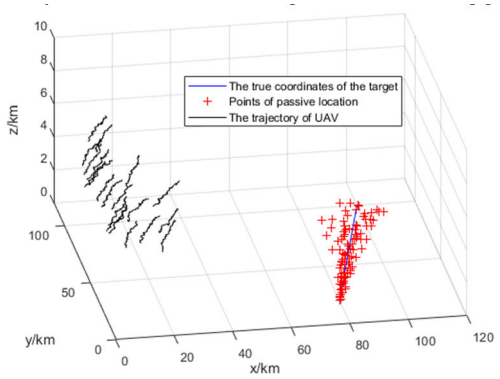

(a) 3D trajectory optimization results

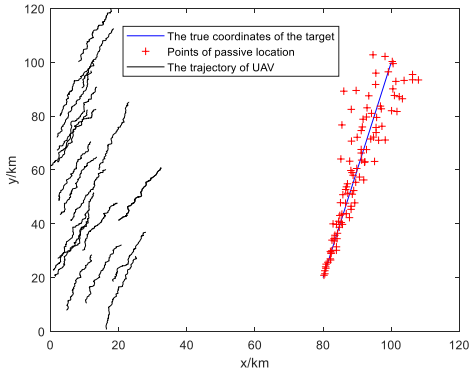

(b) Top view of optimization results

FIGURE 10. Optimization results of the algorithm in literature [30].

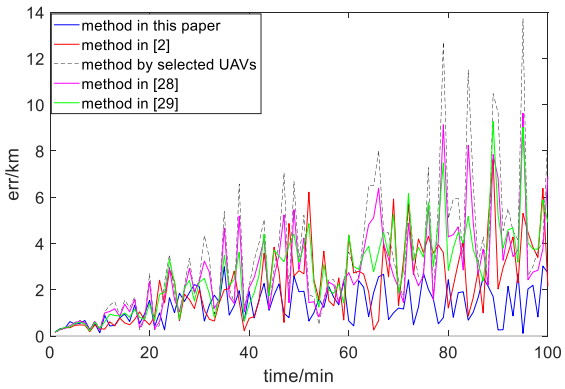

FIGURE 11. Comparison of average errors.

ideal. While, from the perspective of practical application, this method only needs to specify the UAV and does not involve the optimal scheduling of resources, which is simple and easy to implement.

Then take the mean value of each curve in Figure 11, and the results are shown in Table 1.

As can be seen from table 1, the error of the algorithm in this paper is reduced by 60.23%, 45.37%, 51.46 and 52.47% respectively compared with the other four methods. This is because this algorithm always selects the optimal combination of UAVs in the cluster, so as to obtain good positioning effect.

TABLE 1. Comparison of algorithm errors.

Method	Average error /km
Method in this paper	1.3943
Method in [2]	2.4698
Method by selected UAVs	3.3925
Method in [28]	2.7796
Method in [29]	2.8314

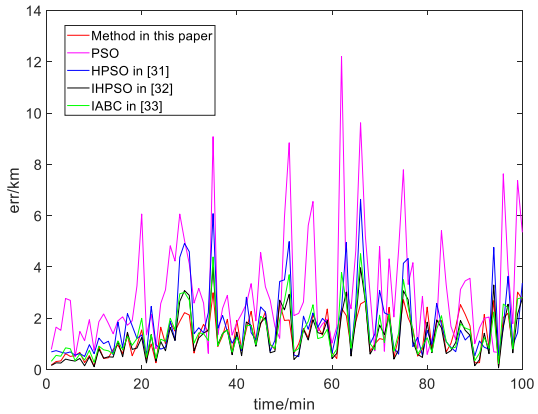

FIGURE 12. Error comparison chart.

B. OPTIMIZATION ALGORITHM PERFORMANCE COMPARISON

In order to further measure and compare the performance of the improved PSO algorithm. The algorithm in this paper is compared with the classical PSO algorithm, the Holonic-PSO (HPSO) in literature [31], the improved Holonic-PSO (IHPSO) in literature [32], and the improved artificial bee colony algorithm (IABC) in literature [33]. The simulation conditions are the same, and 50 Monte Carlo simulations are performed to obtain a comparison chart of the mean error value, as shown in Figure 12.

From Figure 12, it can be seen that the proposed method has better optimization results compared to the classic PSO algorithm. This is because in the subsequent iterations of this article, the optimization results of the pre-time were considered and result inheritance was implemented. In this way, the subsequent results will not be significantly weaker than the previous results, and there will be no prominent purple line in Figure 12. These points are caused by the convergence of the PSO algorithm to local optima, and the method proposed in this paper reduces the possibility of such situations occurring.

It can be seen from Figure 12 that the performance of the algorithm in this paper is inferior to that of HPSO and IHPSO algorithms in terms of optimal times. But the optimization result is close to the best optimal result. At the same time, the method in this paper inherits the results of the previous sequence time. Such iteration is more stable. It can also be

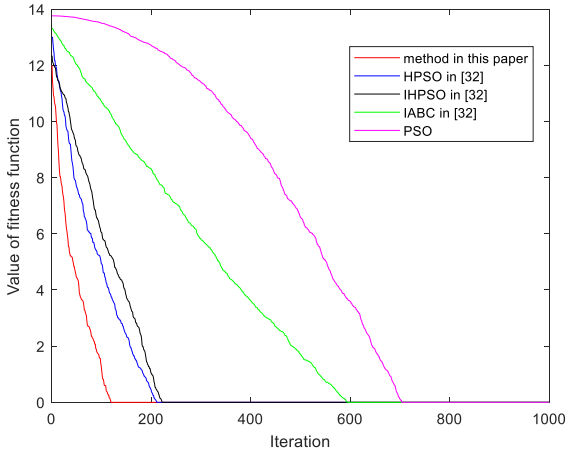

FIGURE 13. Comparison curve of algorithm convergence of F7.

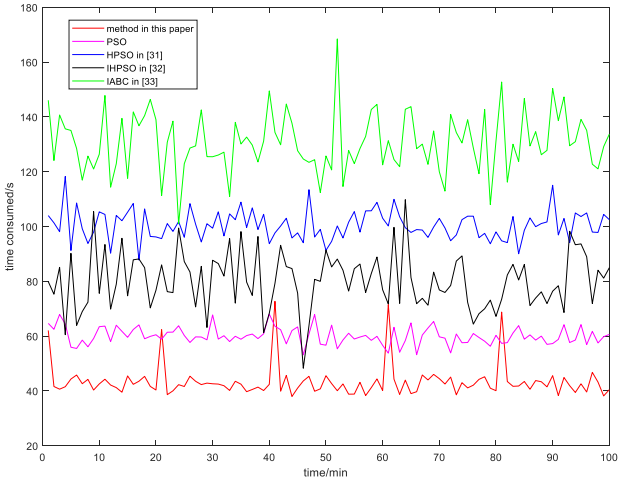

FIGURE 14. Comparison chart of algorithm time consumption.

seen from Figure 12 that the red line is more stable than the blue and the black one.

At the same time, we can also see that the performance of this method is slightly better than IABC algorithm. This is because the literature [33] mainly optimizes the search direction of bees and the selection method of some parameters of the population, and the improvement of the internal search strategy is limited.

In order to further compare the performance of the algorithm, the experimental results in literature [31] and the previous work of the author [32] are combined. The 10 standard benchmark functions F1-F10 in Annex A of document [31] are used to further compare the performance of the algorithm. These ten functions include four types: unimodal, shifted rotated unimodal, multimodal and shifted rotated multi modal, which have good testing ability.

After 50 Monte Carlo simulations of the above five algorithms, the comparison results are shown in Table 2 and Figure 13.

It can be seen from the results in Table 2 and Figure 13 that the method proposed in this paper can find the optimal solution. For some complex functions, the results are weaker than those of HPSO and IHPSO, but the results are close to those of the two methods, and there is no difference in order of magnitude. This is because this algorithm optimizes the particle position at the next moment to ensure the cumulative growth of the efficiency of the algorithm. The optimization result is used as the initial state of the next time, which improves the efficiency of the algorithm. This makes the results of the above 50 Monte Carlo simulation experiments cumulative. Compared with HPSO and IHPSO, which are independent experiments each time, the proposed method has approximate optimization efficiency.

It can also be seen from Figure 13 that the fitness function of the algorithm in this paper decreases the fastest. This is because the improved iterative function has the guidance of the previous optimal parameters, which can make the algorithm converge quickly.

The improvement of PSO in this article mainly focuses on algorithm speed. Perform 50 Monte Carlo experiments and calculate the average algorithm time, and the results are shown in Figure 14.

From Figure 14, it can be seen that the method proposed in this paper takes the shortest time. The PSO algorithm has the fastest single iteration among all intelligent algorithms. However, due to the fact that the classic PSO algorithm requires P iterations to complete. The algorithm in this article requires more computation in a single iteration than the classic PSO algorithm. However, due to the setting of result inheritance and adaptive termination conditions, the algorithm can stop before running P times. Basically, it stopped when it ran to $0.68P$. Significantly improved the speed of the algorithm.

The HPSO algorithm in literature [32] sets the level of particles, and each iteration involves information interaction between groups. Therefore, its algorithm is more time-consuming than PSO. IHPSO in literature [32] adjusted the particle grouping strategy and designed adaptive termination conditions on the basis of HPSO. When the algorithm meets the termination conditions, it will stop searching, so the algorithm time-consuming jitter is large, even lower than the classic PSO sometimes. However, IHPSO algorithm also involves the information interaction between levels. As a result, the computational complexity of its single iteration is significantly higher than that of the classical PSO algorithm. Therefore, the time consumption of the algorithm is higher than that of the classical PSO algorithm.

Because the classic PSO algorithm is recognized as the fastest intelligent algorithm. ABC algorithm is slower than PSO. Literature [33] mainly optimizes the search strategy and population parameters of ABC algorithm, and has no measures to promote its algorithm speed. Therefore, the IABC algorithm in document [33] is slower than ABC and PSO.

Through the above comparison, it can be seen that the improved PSO algorithm in this article is not inferior to mainstream algorithms in terms of optimization accuracy, and

TABLE 2. Evaluation results on ten functions (F1-F10, D =10).

Test Function	Performance	Method in this paper	HPSO	AHPSO	IABC	PSO
F1	Mean	0	0	0	0	0
	Std	0	0	0	0	0
	Median	0	0	0	0	0
F2	Mean	0	0	0	0	0
	Std	0	0	0	0	0
	Median	0	0	0	0	0
F3	Mean	0	0	0	0	0
	Std	0	0	0	0	0
	Median	0	0	0	0	0
F4	Mean	2.4785E+4	2.0268E+4	2.0784E+4	2.861E+4	1.5145E+5
	Std	2.4282E+4	1.7830E+4	1.4281E+4	1.9987E+4	2.6582E+5
	Median	2.5287E+4	1.1023E+4	1.2874E+4	2.7140E+4	3.3363E+4
F5	Mean	0	0	0	0	1.4948E+2
	Std	0	0	0	0	5.7686E+2
	Median	0	0	0	0	1.2449E+3
F6	Mean	0.0036	0.0013	0.0079	0.07185	0.5008
	Std	0.0043	0.0008	0.0016	0.7872	0.7536
	Median	0.0024	0.0011	0.0019	0.8956	0.3074
F7	Mean	0	0	0	0	0
	Std	0	0	0	0	0
	Median	0	0	0	0	0
F8	Mean	0.0239	0.0173	0.0159	0.7017	0.0486
	Std	0.0284	0.0122	0.0099	1.1471	0.0227
	Median	0.0231	0.0185	0.0123	0.6815	0.0492
F9	Mean	0	0	0	0	0.8955
	Std	0	0	0	0	0.9547
	Median	0	0	0	0	0.9949
F10	Mean	1.1013	0.7247	0.5871	0.8023	1.8199
	Std	1.0523	0.7319	0.6118	1.1811	1.2176
	Median	1.0029	0.6590	0.5101	0.7912	1.8488

is more stable. Its algorithm speed is significantly better than other algorithms. At the same time, the method constructed in this article has a good reference value for solving similar time series decision-making problems.

VI. CONCLUSION

This article constructs a passive localization method for unmanned aerial vehicle clusters based on TDOA, providing an algorithm flow for real-time selection of unmanned aerial vehicles for localization and optimization of their spatial positions in the cluster. Firstly, by constructing a TDOA positioning model, the main factors affecting positioning were sorted and analyzed. Afterwards, an objective function for drone selection and trajectory optimization was constructed, and corresponding constraint conditions were constructed. Considering that the real-time trajectory planning problem of unmanned aerial vehicles is a continuous time decision-making problem, where the solutions at adjacent times are relatively similar. We constructed a similarity based result inheritance method and provided an algorithm optimization process. Then sort out the two characteristics of the problem to be optimized, and improve the PSO algorithm based on this. Finally, the advantages of the method were demonstrated through simulation experiments and algorithm comparisons.

REFERENCES

[1] J. Tang, X. Chen, X. Zhu, and F. Zhu, "Dynamic reallocation model of multiple unmanned aerial vehicle tasks in emergent adjustment scenarios," *IEEE Trans. Aerosp. Electron. Syst.*, vol. 59, no. 2, pp. 1139–1155, Apr. 2023.

[2] L. Hao, F. Xiangyu, and S. Manhong, "Research on the cooperative passive location of moving targets based on improved particle swarm optimization," *Drones*, vol. 7, no. 4, p. 264, Apr. 2023, doi: 10.3390/drones7040264.

[3] S. D. Chitte, S. Dasgupta, and Z. Ding, "Distance estimation from received signal strength under log-normal shadowing: Bias and variance," *IEEE Signal Process. Lett.*, vol. 16, no. 3, pp. 216–218, Mar. 2009, doi: 10.1109/LSP.2008.2012229.

[4] Y.-Y. Cheng and Y.-Y. Lin, "A new received signal strength based location estimation scheme for wireless sensor network," *IEEE Trans. Consum. Electron.*, vol. 55, no. 3, pp. 1295–1299, Aug. 2009, doi: 10.1109/TCE.2009.5277991.

[5] Y. Zhao, D. Hu, Z. Liu, and Y. Zhao, "Calibrating the transmitter and receiver location errors for moving target localization in multistatic passive radar," *IEEE Access*, vol. 7, pp. 118173–118187, 2019, doi: 10.1109/ACCESS.2019.2932748.

[6] B. Li, K. Zhao, and X. Shen, "Dilution of precision in positioning systems using both angle of arrival and time of arrival measurements," *IEEE Access*, vol. 8, pp. 192506–192516, 2020, doi: 10.1109/ACCESS.2020.3033281.

[7] H.-W. Wei and S.-F. Ye, "Comments on 'A linear closed-form algorithm for source localization from time-differences of arrival,'" *IEEE Signal Process. Lett.*, vol. 15, p. 895, 2008, doi: 10.1109/LSP.2008.2001113.

[8] S. Abeywickrama, T. Samarasinghe, C. K. Ho, and C. Yuen, "Wireless energy beamforming using received signal strength indicator feedback," *IEEE Trans. Signal Process.*, vol. 66, no. 1, pp. 224–235, Jan. 2018, doi: 10.1109/TSP.2017.2764854.

[9] A. Maric, E. Kaljic, P. Njemcevic, and V. Lipovac, "Projective approach in determining homogeneous hyperspherical geometrically-based stochastic channel model's statistics: Angle of departure, angle of arrival and time of arrival," *IEEE Trans. Wireless Commun.*, vol. 19, no. 12, pp. 7864–7880, Dec. 2020, doi: 10.1109/TWC.2020.3017154.

[10] H. Xu, Y. Zhang, B. Ba, D. Wang, and X. Li, "Fast joint estimation of time of arrival and angle of arrival in complex multipath environment using OFDM," *IEEE Access*, vol. 6, pp. 60613–60621, 2018, doi: 10.1109/ACCESS.2018.2875824.

[11] G. H. Wang, J. Bai, Y. He, and J. J. Xiu, "Optimal deployment of multiple passive sensors in the sense of minimum concentration ellipse," *IET Radar, Sonar Navigat.*, vol. 3, no. 1, pp. 8–17, Feb. 2009.
[12] W. Huihui, Z. Xingqun, and Z. Yanhua, "Geometric dilution of precision for GPS single-point positioning based on four satellites," *J. Syst. Eng. Electron.*, vol. 19, no. 5, pp. 1058–1063, Oct. 2008.
[13] J. Schloemann, H. S. Dhillon, and R. M. Buehrer, "A tractable metric for evaluating base station geometries in cellular network localization," *IEEE Wireless Commun. Lett.*, vol. 5, no. 2, pp. 140–143, Apr. 2016.
[14] I. Sharp, K. Yu, and Y. Jay Guo, "GDOP analysis for positioning system design," *IEEE Trans. Veh. Technol.*, vol. 58, no. 7, pp. 3371–3382, Sep. 2009.
[15] M. Zoghi and M. H. Kahaei, "Adaptive sensor selection in wireless sensor networks for target tracking," *IET Signal Process.*, vol. 4, no. 5, pp. 530–536, Oct. 2010.
[16] H. Godrich, A. M. Haimovich, and R. S. Blum, "Target localisation techniques and tools for multiple-input multiple-output radar," *IET Radar, Sonar Navigat.*, vol. 3, no. 4, pp. 314–327, Aug. 2009.
[17] B. Yang and J. Scheuing, "A theoretical analysis of 2D sensor arrays for TDOA based localization," in *Proc. IEEE Int. Conf. Acoust. Speed Signal Process.*, May 2006, pp. 901–904.
[18] K. W. K. Lui and H. C. So, "A study of two-dimensional sensor placement using time-difference-of-arrival measurements," *Digit. Signal Process.*, vol. 19, no. 4, pp. 650–659, Jul. 2009.
[19] Q. He, R. S. Blum, H. Godrich, and A. M. Haimovich, "Target velocity estimation and antenna placement for MIMO radar with widely separated antennas," *IEEE J. Sel. Topics Signal Process.*, vol. 4, no. 1, pp. 79–100, Feb. 2010.
[20] Q. He, J. Hu, R. S. Blum, and Y. Wu, "Generalized Cramér–Rao bound for joint estimation of target position and velocity for active and passive radar networks," *IEEE Trans. Signal Process.*, vol. 64, no. 8, pp. 2078–2089, Dec. 2015.
[21] O. Cakir, I. Kaya, A. Yazgan, and Ö. Cakir, "Dynamic orientation of receiver arrays using particle swarm optimisation," *Electron. Lett.*, vol. 49, no. 21, pp. 1313–1315, Oct. 2013.
[22] A. N. Bishop, B. Fidan, B. D. O. Anderson, K. Dogancay, and P. N. Pathirana, "Optimality analysis of sensor-target geometries in passive localization: Part 1—Bearing-only localization," in *Proc. 3rd Int. Conf. Intell. Sensors, Sensor Netw. Inf.*, Dec. 2007, pp. 7–12.
[23] A. N. Bishop, B. Fidan, B. D. O. Anderson, P. N. Pathirana, and K. Dogancay, "Optimality analysis of sensor-target geometries in passive localization: Part 2—Time-of-arrival based localization," in *Proc. 3rd Int. Conf. Intell. Sensors, Sensor Netw. Inf.*, Dec. 2007, pp. 13–18.
[24] S. E. Ferik and O. R. Thompson, "Biologically inspired control of a fleet of UAVs with threat evasion strategy," *Asian J. Control*, vol. 19, no. 1, pp. 1–18, 2017.
[25] N. Okello, F. Fletcher, D. Musicki, and B. Ristic, "Comparison of recursive algorithms for emitter localisation using TDOA measurements from a pair of UAVs," *IEEE Trans. Aerosp. Electron. Syst.*, vol. 47, no. 3, pp. 1723–1732, Jul. 2011.
[26] S. A. A. Shahidian and H. Soltanizadeh, "Optimal trajectories for two UAVs in localization ofmultiple RF sources," *Trans. Inst. Meas. Control*, vol. 38, no. 8, pp. 908–916, 2015.
[27] F. Koohifar, A. Kumbhar, and I. Guvenc, "Receding horizon multi-UAV cooperative tracking of moving RF source," *IEEE Commun. Lett.*, vol. 21, no. 6, pp. 1433–1436, Jun. 2017.
[28] J. Tang, G. Liu, and Q. Pan, "A review on representative swarm intelligence algorithms for solving optimization problems: Applications and trends," *IEEE/CAA J. Autom. Sinica*, vol. 8, no. 10, pp. 1627–1643, Oct. 2021.
[29] Z. Yongsheng, H. Dexiu, Z. Yongjun, and L. Zhixin, "Moving target localization for multistatic passive radar using delay, Doppler and Doppler rate measurements," *J. Syst. Eng. Electron.*, vol. 31, no. 5, pp. 939–949, Oct. 2020, doi: 10.23919/JSEE.2020.000071.
[30] X. Cheng, F. Shu, Y. Li, Z. Zhuang, D. Wu, and J. Wang, "Optimal measurement of drone swarm in RSS-based passive localization with region constraints," *IEEE Open J. Veh. Technol.*, vol. 4, pp. 1–11, 2023, doi: 10.1109/OJVT.2022.3213866.
[31] M. Roshanzamir, M. A. Balafar, and S. N. Razavi, "Empowering particle swarm optimization algorithm using multi agents' capability: A holonic approach," *Knowl.-Based Syst.*, vol. 136, pp. 58–74, Nov. 2017.
[32] H. Li, H. Jin, H. Wang, and Y. Ma, "Improved adaptive holonic particle swarm optimization," *Math. Problems Eng.*, vol. 2019, pp. 1–22, Dec. 2019.
[33] X. Fan, P. Bai, H. Wang, J. Zhang, and H. Li, "Joint optimization method of airborne MIMO radar track and radiated power based on mutual information," *IEEE Access*, vol. 8, pp. 136278–136295, 2020.

LEI SHENG was born in 1994. He received the B.Eng. degree in optoelectronics information and science from the Changchun University of Science and Technology, Changchun, China.

His research interests are UAV swarm, flight control, and intelligence algorithms. He has participated in several National Natural Science Foundation.

HAO LI was born in 1981. He received the B.Eng. degree in radar engineering and the M.Eng. degree in information and communication engineering from the Radar Academy, Wuhan, China, and the Ph.D. degree in electronic science and technology from Engineering University, Xi'an, China, in 2017.

He has published more than 20 journal articles as the major author, among them, 12 articles were retrieved by SCI/EI. He has hosted and participated in several National Natural Science Foundation. His current research interests are swarm intelligence, UAV swarm, intelligence systems, and signal processing.

YINGCHUAN QI was born in 1965. He received the B.S. and M.S. degrees in electric power transmission and automation from the China University of Mining and Technology, in 1992, and the Ph.D. degree in intelligent control from the Wuhan University of Technology, Wuhan, China.

He is the author of four books and more than 60 articles. His research interests include UAV control technology and application, power electronics, and transmission and flight control.

MANHONG SHI was born in 1976. He received the M.Eng. degree in navigation, guidance, and control from Engineering University, Xi'an, China, in 2006.

His current research interests are swarm intelligence, UAV swarm, aircraft design, and flight control. He has published more than 20 journal articles as the major author, among them, three articles were retrieved by EI.